Research article

Structural parameters are superior to eigenvector centrality in detecting progressive supranuclear palsy with machine learning & multimodal MRI

Franziska Albrecht [a,b,c,1,3,*], Karsten Mueller [a,d,1], Tommaso Ballarini [a], Klaus Fassbender [e], Jens Wiltfang [f,g], FTLD-Consortium [4], Markus Otto [h,i], Robert Jech [d,**,2], Mattias L. Schroeter [a,j,2]

[a] *Max Planck Institute for Human Cognitive and Brain Sciences, Leipzig, Germany*
[b] *Division of Physiotherapy, Department of Neurobiology, Care Sciences and Society, Karolinska Institutet, Stockholm, Sweden*
[c] *Women's Health and Allied Health Professionals Theme, Medical Unit Occupational Therapy & Physiotherapy, Karolinska University Hospital, Stockholm, Sweden*
[d] *Department of Neurology, Charles University, First Faculty of Medicine and General University Hospital, Prague, Czech Republic*
[e] *Department of Neurology, Saarland University, Germany*
[f] *University Medical Center Göttingen, Germany*
[g] *German Center for Neurodegenerative Diseases (DZNE), Göttingen, Germany*
[h] *Department of Neurology, University of Ulm, Ulm, Germany*
[i] *Department of Neurology, Martin Luther University Halle-Wittenberg, Halle (Saale), Germany*
[j] *Clinic of Cognitive Neurology, University of Leipzig, Germany*

ARTICLE INFO

ABSTRACT

Progressive supranuclear palsy (PSP) is an atypical Parkinsonian syndrome characterized initially by falls and eye movement impairment. This multimodal imaging study aimed at eliciting structural and functional disease-specific brain alterations. T1-weighted and resting-state functional MRI were applied in multi-centric cohorts of PSP and matched healthy controls. Midbrain, cerebellum, and cerebellar peduncles showed severely low gray/white matter volume, whereas thinner cortical gray matter was observed in cingulate cortex, medial and temporal gyri, and

* Corresponding author. Max-Planck-Institute for Human Cognitive and Brain Sciences, Stephanstraße 1 A, 04103, Leipzig, Germany
** Corresponding author. Department of Neurology and Center of Clinical Neuroscience, Charles University, First Faculty of Medicine and General University Hospital in Prague, Kateřinská 30, 120 00, Prague, Czech Republic
E-mail address: jech@cesnet.cz (R. Jech).
[1] Authors contributed equally.
[2] Equal senior author contribution.
[3] **Present Address:** Dr. rer. nat. Franziska Albrecht: Karolinska Institutet, Alfred Nobels Allé 23, 141 52 Huddinge, Sweden.
[4] **FTLD-Consortium:** Adrian Danek (LMU München), Janine Diehl-Schmid (TU München), Holger Jahn (Hamburg), Jan Kassubek (Ulm), Johannes Kornhuber (Erlangen), Bernhard Landwehrmeyer (Ulm), Martin Lauer (Würzburg), Johannes Prudlo (Rostock), Anja Schneider (Bonn), Albert C. Ludolph (Ulm), Klaus Fliesbach (Bonn), Sarah Anderl-Straub (Ulm), Katharina Brüggen (Rostock), Marie Fischer (Erlangen), Hans Förstl (TU München), Anke Hammer (Erlangen), György Homola (Würzburg), Walter Just (Ulm), Johannes Levin (LMU München), Nicolai Marroquin (Ulm), Anke Marschhauser (Leipzig), Danielé Pino (Leipzig), Magdalena Nagl (Ulm), Timo Oberstein (Erlangen), Lea Hüper (Leipzig), Maryna Polyakova (Leipzig), Hannah Pellkofer (Göttingen), Tanja Richter-Schmidinger (Erlangen), Carola Rossmeier (TU München), Marianna Kulko (Leipzig), Elisa Semler (Ulm), Annika Spottke (Bonn), Petra Steinacker (Halle (Saale)), Angelika Thöne-Otto (Leipzig), Ingo Uttner (Ulm), and Heike Zech (Göttingen).

insula. Eigenvector centrality analyses revealed regionally specific alterations. Multivariate pattern recognition classified patients correctly based on gray and white matter segmentations with up to 98 % accuracy. Highest accuracies were obtained when restricting feature selection to the midbrain. Eigenvector centrality indices yielded an accuracy around 70 % in this comparison; however, this result did not reach significance. In sum, the study reveals multimodal, widespread brain changes in addition to the well-known midbrain atrophy in PSP. Alterations in brain structure seem to be superior to eigenvector centrality parameters, in particular for prediction with machine learning approaches.

1. Introduction

Progressive supranuclear palsy (PSP) is a rare atypical Parkinsonian syndrome that shares several features with the more common idiopathic Parkinson's disease, making it challenging to diagnose. PSP progresses more rapidly and from the early disease stage on involves backward falls as well as impairment of eye movements known as gaze palsy; differentiating it clinically from other neurodegenerative diseases [1].

Diagnostic criteria were recently amended. Still, the diagnosis of PSP remains primarily dependent on clinical evaluation, with neuroimaging considered a criterion to support diagnosis, i.e., 'predominant midbrain atrophy or hypometabolism' [1]. Recently, we conducted a comprehensive, whole-brain, systematic and quantitative meta-analysis based on anatomical likelihood estimation to extract disease-specific neural networks [2]. We identified structural changes in the gray matter in the bilateral thalamus, anterior insulae, midbrain, and left caudate nucleus. The included studies converged in the white matter, specifically in bilateral superior/middle cerebellar pedunculi, cerebral pedunculi, and midbrain. In subtraction analyses, the midbrain was identified as differentiating between PSP and Parkinson's disease. These findings were supported by region-of-interest effect size meta-analyses. Thus, atrophy in the midbrain and cerebral/cerebellar pedunculi was identified as a potential disease-characteristic feature of PSP that might be regarded as a pathognomonic marker. Nevertheless, further validation in an independent cohort is needed to support disease-specificity. Further, to strengthen disease understanding and comprehensively describe brain alterations, studies should integrate multimodal whole-brain imaging approaches.

Resting-state functional connectivity studies in PSP have, to date, covered selective connectivity approaches like seed-based analyses. Seeds were placed according to *a priori* hypothesis in regions shown to be affected by PSP such as the midbrain, cerebellum, and thalamus [3–6]. Decreased functional connectivity was mainly observed, with a few increases between the regions. A data-driven approach that investigates unbiased functional connectivity changes in PSP, without *a priori* selected networks, is still missing. Such an unbiased approach may reveal further information on which areas are involved in PSP.

In recent years, machine learning techniques have gained prominence in various fields, including medical research and diagnostics. Among these techniques, Support-vector Machine classification (SVM) stands out as a powerful tool for classification tasks. SVM is a supervised learning algorithm that aims to find an optimal hyperplane to separate data points into distinct classes. It maximizes the margin between classes, allowing for robust classification. SVM has been successfully applied to distinguish patients with specific medical conditions from healthy individuals, paving the way to aid in early diagnosis and personalized treatment strategies [7]. Neurodegenerative disorders, such as Alzheimer's disease, Parkinson's disease, and progressive supranuclear palsy (PSP), present complex clinical manifestations. SVM, when applied to neuroimaging data (e.g., MRI scans), can identify subtle patterns associated with these disorders [7]. Distinguishing PSP patients from healthy controls based on clinical symptoms alone can be challenging. SVM, leveraging neuroanatomical features extracted from brain imaging, offers a promising avenue for accurate classification.

In the present study we applied multimodal neuroimaging including structural and resting-state functional magnetic resonance imaging (MRI) to identify the neural correlates of PSP. Multicentric data were acquired through the FTLD Consortium Germany and Charles University in Prague, Czech Republic. With voxel-based and surface-based morphometry, we investigated structural alterations related to PSP. Whole-brain functional connectivity changes were assessed by eigenvector centrality mapping (ECM). We additionally applied a seed-based approach using brain regions identified as atrophic and prototypical for the disease in our recent meta-analysis [2]. Of note, this meta-analysis did not include data from the present study, and, accordingly, seeds of interest are defined in a totally independent cohort, avoiding circularity. With a multivariate pattern recognition approach (SVM), we examined which patterns and regions contribute the most to distinguishing patients with PSP from controls. Based on the nature of PSP and, on prior results we hypothesized multimodal brain alterations in the midbrain, thalami, insulae, caudate nuclei, and cerebellar/cerebral pedunculi to contribute to the identification of PSP patients.

2. Materials and methods

2.1. Study participants

Multicentric data were included from the German Consortium of Frontotemporal Lobar Degeneration (FTLD-Consortium) Germany and from the Department of Neurology, Charles University of Prague, Czech Republic. Patients were diagnosed by experienced neurologists at the respective study centers. Twenty-two PSP patients were compared with 22 age-, sex-, and scanner-matched healthy controls (Table 1). Missing data for the Mini Mental State Examination has been replaced by the mean value (MMSE, N = 5). Pearson's

Chi-Squared test (χ^2) and unpaired Student's T-tests indicated no significant differences between the cohorts concerning demographic variables (Table 1). The study was approved by the ethics committees of the General University Hospital in Prague and the University of Leipzig (ID137-11-18042011). Participants were fully informed and gave written consent in accordance with the Declaration of Helsinki.

2.2. Image acquisition and preprocessing

High-resolution T1-weighted structural brain images were obtained with 3T MAGNETOM scanners (Siemens, Erlangen, Germany) using the magnetization-prepared rapid gradient-echo (MP-RAGE) sequence. In addition, functional images (so-called "resting-state" functional MRI, or short rs-fMRI) were acquired using gradient echo echo-planar imaging (EPI) at each center (see Supplemental Table 1 in osf.io/yan47/). All rs-fMRI scans were acquired with a repetition time (TR) of 2 s, an echo time (TE) of 30 ms, and a spatial resolution of 3 mm which was not changed during image preprocessing with spatial normalization, i.e., the entire analysis was based on a 3 mm spatial resolution [8,9]. All rs-fMRI scans were acquired with a minimum length of 300 functional volumes which was consistently used in all analyses, thus, the temporal length of the resting-state fMRI scan we used in the analysis was about 10 min. Note that the total scanning time varied from patient to patient due to clinical needs. Participants had their eyes closed during scanning. MRI data were processed using SPM12 (rev.12.7771), CAT12 (12.2), FSL (v. 5.0.9), and Matlab R2024a (24.1.0).

2.3. Voxel-based morphometry

Voxel-based morphometry was performed with the CAT12 toolbox [10]. During preprocessing, images were spatially normalized with the standard stereotactic space of the Montreal Neurological Institute (MNI), segmented using tissue probability maps for gray matter, white matter, and cerebrospinal fluid (CSF), modulated by the amount of non-linear deformation, and smoothed with a Gaussian kernel of 8 mm full width at half-maximum. Voxel-wise *t*-tests were performed to compare PSP patients with controls. Covariates were used to control for age, gender, and total intracranial volume. Clusters were detected using an initial voxel threshold of $P < 0.005$. To correct for multiple comparisons, significant results were obtained using family-wise error (FWE) correction with $P < 0.05$ at the cluster-level.

2.4. Surface-based morphometry

We applied the default preprocessing pipeline according to the recommendations of CAT12 with an initial threshold of $P < 0.005$ and an extent threshold of $k > 300$ vertices. To control for multiple comparisons, FWE correction was performed with $P < 0.05$ at the cluster-level.

2.5. Resting-state functional connectivity

Standard SPM preprocessing was applied to rs-fMRI data including the following steps: realignment with rigid co-registration of functional volumes, slice-time correction with the middle slice as a reference, spatial normalization with the MNI space, bias field correction, and unified segmentation. Images were smoothed with a Gaussian kernel of full-width-half-maximum 8 mm to balance the signal-to-noise ratio. Nuisance regression variables included six motion parameters from the SPM realignment output and mean

Table 1
Demographic data and scanner characteristics for patients with progressive supranuclear palsy (PSP) and healthy controls (HC).

Cohort	Subject group	Age (years)	Sex (female/male)	Disease duration (years)	MMSE	Scanner Model
FTLD	PSP	73.14 ± 10.98	3/4	5.70 ± 5.70	25.29 ± 4.00	Prisma 3, Skyra 2, TrioTim 1, Verio 1
	HC	70.00 ± 8.2	3/4			Prisma 3, Skyra 2, TrioTim 1, Verio 1
Prague	PSP	65.87 ± 5.53	5/10	5.10 ± 4.40	25.10 ± 3.41	TrioTim 9, Skyra 6
	HC	65.80 ± 6.66	4/11			TrioTim 9, Skyra 6
All	PSP	68.18 ± 8.17	7/15	5.3 ± 4.71	25.18 ± 3.56	Prisma 3, Skyra 8, TrioTim 10, Verio 1
	HC	67.14 ± 7.27	8/14			Prisma 3, Skyra 8, TrioTim 10, Verio 1
Statistical differences						
FTLD vs. Prague		t = 2.08, df = 18, $p = 0.052$	χ [2] = 0.25, df = 1, $p = 0.620$	t = 0.25, df = 9.44, $p = 0.81$	t = 0.099, df = 11.59, $p = 0.92$	
PSP vs. HC		t = 0.45, df = 41.4, $p = 0.66$	χ [2] = 1, df = 1, $p = 1$			

Mean ± standard deviation. Student's *T*-test was applied to compare numerical variables and χ^2 test to compare categorical variables across groups. Scanner model specifies the manufacturer model and the number of participants assessed using the scanner. Abbreviations: HC healthy controls, MMSE Mini Mental State Examination, PSP progressive supranuclear palsy.

intensity signals provided by the anatomical segmentation of white matter and cerebrospinal fluid based on each subject's structural MRI. High-pass filtering of 0.0125 Hz was applied to remove linear baseline drifts and low-frequency noise. Measurements of framewise-displacement (FD) [11] were computed for each subject separately to check for head motion: mean FD, maximum FD, and maximum FD after discarding the largest 5 % of the FD. Resulting head motion parameters were compared for each measure between the cohorts from the two centers as well as between patients and controls, applying independent sample *t*-tests.

2.6. Eigenvector centrality mapping

To explore whole-brain functional connectivity in complex networks, we implemented the graph-theory method of Eigenvector Centrality Mapping (ECM). The importance of functional brain hubs is weighted based on their connectedness with other heavily connected nodes. ECM was computed using LIPSIA software [12]. For the analyses, a mask was created by combining the tissue probability map from SPM (smoothed with 8 mm and thresholded at 0.2 to obtain an inclusive mask) and the functional images from patients and controls. This ensured that only voxels containing functional data were included in the analyses.

Since blood-oxygen-level dependent (BOLD) time courses between voxels can be positively and negatively correlated, LIPSIA offers several approaches to account for this. Negative correlations do not fulfill the requirements of the Perron-Frobenius theorem (i.e., obtaining the unique largest eigenvalue is only possible in a symmetric, positive similarity matrix) [13], while calculation and biological meaning of these negative correlations are still under debate [14,15]. Hence, we only discuss the positive correlations and report the remaining approaches (integrating negative correlations) on the OSF (osf.io/yan47/). ECM analysis results in one 3D map per subject, where each voxel represents its eigenvector centrality value.

T-tests were performed to identify clusters with significant intrinsic functional connectivity differences between controls and patients with PSP. Statistical parametric maps were processed with an initial threshold of $P < 0.005$ and a spatial threshold of $k > 200$ voxels. To correct for multiple comparisons, significant clusters were obtained using FWE correction with $P < 0.05$ at the cluster level.

2.7. Seed-based functional connectivity

To test selective functional connectivity changes in PSP, we used the peaks of the significant clusters from our recent meta-analysis [2] as seeds. Thus, the analysis was focused on disease-specific regions as hubs of interest. We ran seed-based analysis in Matlab with our custom-developed script. Extracted BOLD time courses from the seeds were correlated with the time courses of all other voxels in the brain. For each subject the resulting map consisted of voxel-wise correlation coefficients with the seeds. Based on the meta-analysis, we used the right thalamus (8 -12 16, x y z, MNI), left thalamus (-2 -24 6), left insula (-38 14 2), right insula (44 18 4), left caudate nucleus (-10 6 12), and midbrain (0 -18 -8) as seeds and mapped functional connectivity to other brain regions. We tested between-group differences in a two-sample *t*-test in SPM12 applying the same approach as used with the ECM analysis, i.e., using an initial threshold of $P < 0.005$ with an extent threshold of $k > 200$ voxels. Significant clusters were obtained using FWE correction with $P < 0.05$ at the cluster-level.

2.8. Support vector machine classification

Using PRoNTo (v2.1) [16] we explored individual disease prediction by MRI. Multivariate patterns were considered rather than voxel-wise comparisons as in the aforementioned studies. We classified structural (gray and white matter volume) and rs-fMRI (ECM) modalities. Additionally, classification was performed using a restricted feature selection including white matter within the midbrain using the WFU PickAtlas (version 3.0.5b). Included features for each classifier were for gray matter 522135 voxels, white matter 279662 voxels, midbrain 14947 voxels, and ECM 66906 voxels. Leave-one-per-group-out cross-validation was performed to build the classifier. Classification results were obtained with 10,000 permutations. Significant results were obtained with $P < 0.005$. To display the classification results, relative weights of the contribution of each voxel to the classification were calculated. The cross-validation schemes and the confusion matrices can be found on our OSF page (see PRoNTo.zip in osf.io/yan47/).

2.9. Sensitivity analysis

All neuroimaging analyses have been performed adding a site covariate (Prague vs. FTLD consortium), disease duration, and MMSE as additional covariates as sensitivity analysis. In addition, we also investigated a potential sex effect investigating the amount of variance that can be explained by the sex covariate using an *F*-test. However, these sensitivity analyses did not lead to substantial changes in our results, which is why we do not report them in the main text. Nevertheless, all analyses are publicly available via the OSF (osf.io/yan47/).

2.10. Data availability

Individual gray and white matter maps (VBM), cortical thickness maps, seed-based correlation maps, and ECM maps have been uploaded to the OSF (osf.io/yan47/). This includes ensuring that the code is well-documented (including additional batch and README files), and that any dependencies or data privacy concerns are appropriately addressed. All statistical (SPM) and classification (PRoNTo) analyses reported in this manuscript are available and can be reproduced using our OSF repository. The original datasets are available upon reasonable request. Data of participants are stored at the FTLD-Consortium and the Charles University in

Prague. Patients' data must maintain confidentiality and, accordingly, are only shared at reasonable request to replicate procedures and analyses of the study in line with the implementation of the General Data Protection Regulation (GDPR).

2.11. Visualization

Statistical results were exported from SPM12 saving the thresholded statistical parametric maps as NIfTI images. Figures showing orthogonal brain slices were generated using the Mango software (Research Imaging Institute, University of Texas Health Science Center) with the 'Overlay' and the 'Parametric Overlay' function, respectively. Glass brain views were generated using the nilearn package with python. Note that, prior to visualization, all rs-fMRI results were resampled to match the resolution of the underlying anatomical image within the MNI space. Brain surface representations were obtained using the 'Surface Overlay' of the CAT toolbox and the FsAverage template.

3. Results

3.1. Voxel-based morphometry

Reduced gray matter volume in bilateral hemispheres was apparent in the thalamus, insula, anterior/middle cingulate cortex, cerebellum, cuneus, middle occipital gyrus, temporal gyrus, frontal gyrus, and orbital gyrus (Fig. 1 and GM.zip in osf.io/yan47/). White matter volume reductions in patients with PSP were found in both hemispheres in the cingulum spreading to the frontal and orbital gyrus and thalamus/midbrain spreading to cerebellum, encompassing the cerebellar pedunculi (Fig. 1 and WM.zip in osf.io/yan47/).

There was no increased gray or white matter when comparing patients with PSP to controls.

3.2. Surface-based morphometry

Thinner cortical gray matter in patients with PSP was observed in the middle cingulate cortex, superior medial gyrus, superior temporal gyrus, and supramarginal gyrus; all in the left hemisphere (Fig. 2 and CT.zip in sf.io/yan47/ osf.io/yan47/). On the right side, thinner cortex was present in the middle and anterior cingulate cortex, parahippocampal gyrus, entorhinal cortex, fusiform gyrus, insula, and temporal pole.

3.3. Eigenvector centrality mapping

Weaker functional connectivity in patients with PSP was found in both hemispheres in the precuneus, superior parietal lobe,
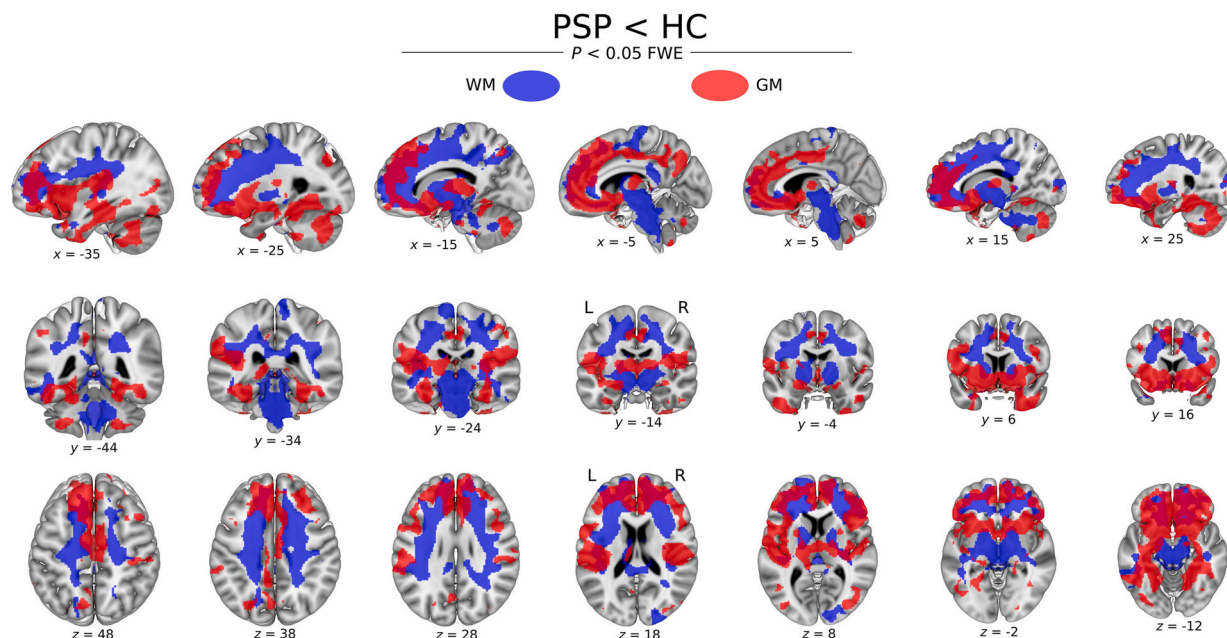
Fig. 1. Structural changes in gray (GM) and white matter (WM) in patients with progressive supranuclear palsy (PSP). Voxel-based morphometry analyses in comparison to matched healthy controls (HC). Slice coordinates (x,y,z) in mm. Abbreviations: FWE family-wise error correction, L left, R right.

CT: PSP < HC

$P < 0.05$ FWE
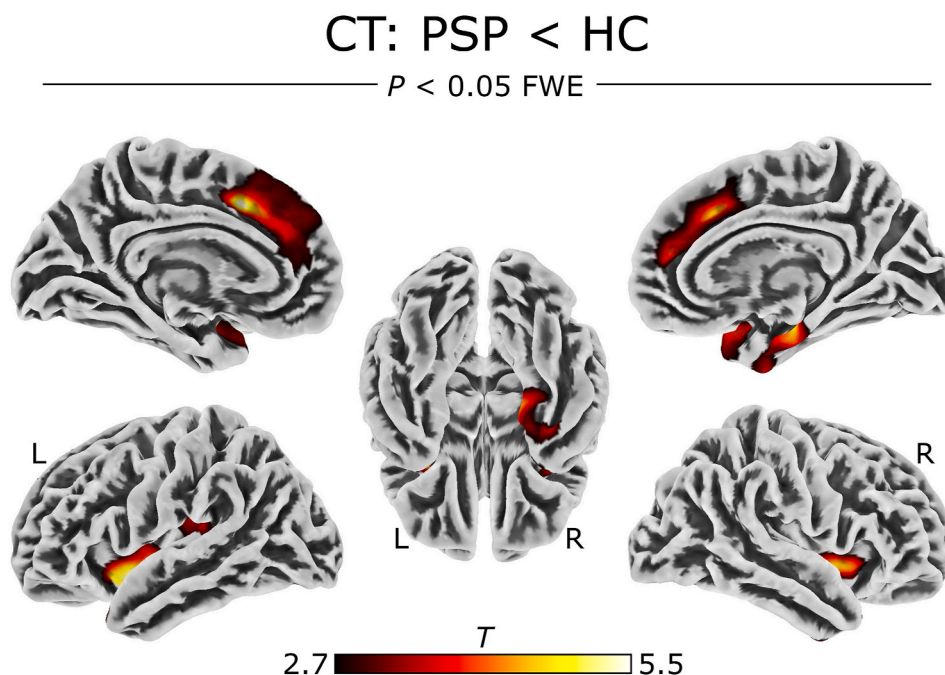
Fig. 2. Surface-based morphometry analysis in patients with progressive supranuclear palsy compared with healthy controls. Thinner cortical thickness (CT) in patients is shown in dark red. Abbreviations: FWE family-wise error correction, L left, R right.

postcentral gyrus, supramarginal gyrus, superior frontal gyrus, and middle cingulate cortex (Fig. 3 and ECM.zip in osf.io/yan47/). Functional connectivity was also weaker in the left pre-/postcentral gyrus, central operculum, and the right middle/inferior frontal gyrus in PSP. Stronger functional connectivity was found in the bilateral anterior cingulate and medial frontal cortices, the left fusiform gyrus, inferior/middle temporal gyrus, and hippocampus. In the right hemisphere, greater connectedness in patients with PSP was seen in the superior/middle frontal gyrus, precentral gyrus, and inferior/middle temporal gyrus.

Additionally, we ran analyses with different approaches that account for negative correlations between time courses in the similarity matrices, which are reported on our OSF repository (osf.io/yan47/). In sum, the resulting patterns were like our main approach of only including positive correlations.

3.4. Seed-based functional connectivity

To investigate disease-specific functional connectivity changes, we additionally applied a seed-based approach focused on brain regions that were identified as atrophic and prototypical for the disease in our recent meta-analysis in a large and independent cohort [2]. The seed in the midbrain showed greater functional connectivity to the left posterior/anterior cingulate gyrus, left medial orbital gyrus, left gyrus rectus/medial frontal gyrus, right thalamus, and right medial frontal/anterior cingulate cortex in PSP compared with controls (Fig. 4). Other seed regions showed a decrease of functional connectivity in PSP compared with controls: The right thalamus seed showed weaker functional connectivity to the left middle/anterior cingulate gyrus, left middle/superior frontal gyrus, right middle cingulate gyrus, right middle frontal gyrus, and right frontal operculum. Weaker functional connectivity with the left insula seed was revealed in the bilateral middle cingulate and left supplementary motor cortex. The right insula seed showed weaker functional connectivity to the bilateral thalamus and left cerebellum (see Fig. 4 and SBC.zip in osf.io/yan47/). No weakened functional connectivity was found for the seed in the midbrain while no stronger functional connectivity was observed for the seeds in the right thalamus and right and left insula. There were no significant functional connectivity changes to the left caudate nucleus and left thalamus.

3.5. Potential impact of head motion on functional results

Of note, motion effects did not have a significant impact on these results. We did not find any differences in mean FD between patients and controls ($t = 0.05$, df $= 40$, $P = 0.96$) or between the Prague and FTLD cohort ($t = -0.98$, df $= 26$, $P = 0.34$) (see also Supplemental Table 2 and Supplemental Figure 1 in osf.io/yan47/). Further, there were no significant differences between maximum FD when discarding 5 % of the highest values (patients/controls: $t = -0.59$, df $= 33$, $P = 0.56$, FTLD/Prague: $t = 0.07$, df $= 39$, $P = 0.94$).
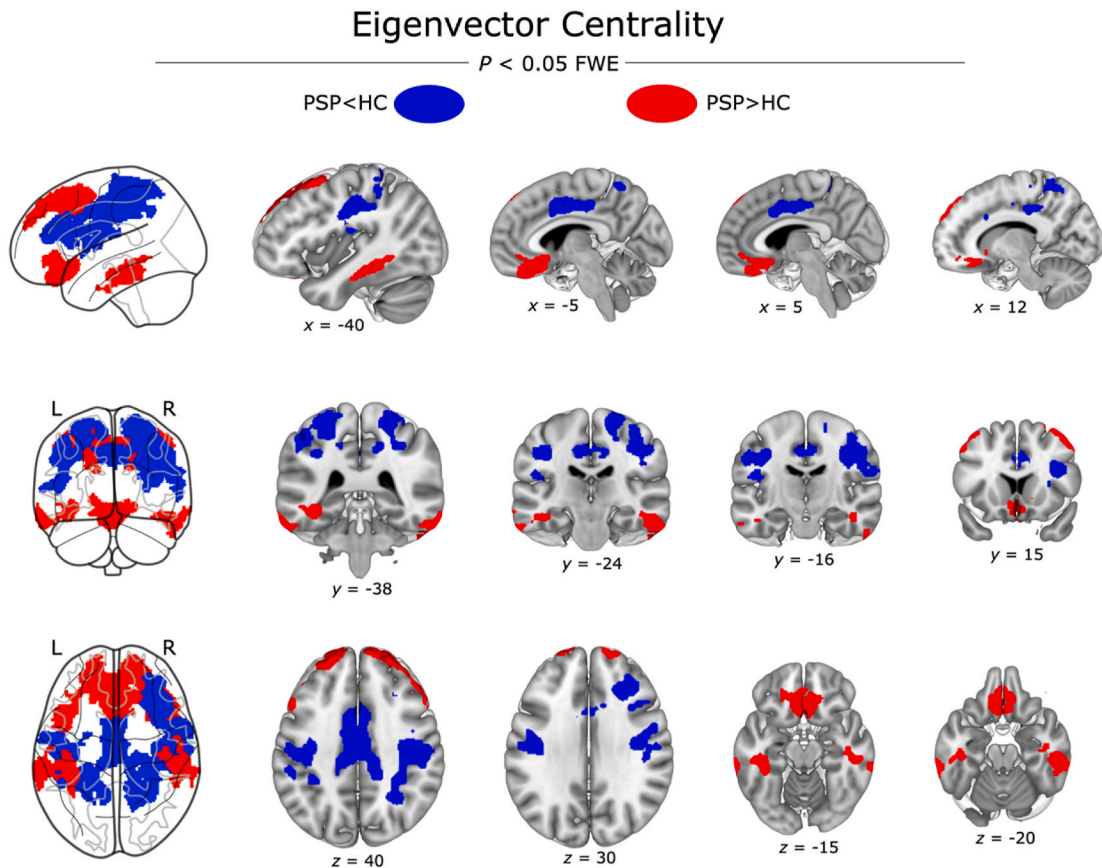
Fig. 3. Eigenvector centrality is stronger and weaker in patients with progressive supranuclear palsy (PSP) compared to healthy controls (HC). Only positive correlations between time courses in the similarity matrices are shown. Slice coordinates (x,y,z) in mm. Abbreviations: FWE family-wise error correction, L left, R right.

3.6. Support vector machine classification to predict PSP

We could reliably identify PSP versus controls using whole-brain gray and white matter (Fig. 5A–B). Patients with PSP were correctly classified relying on the white matter with a total accuracy, sensitivity, and specificity each of 86 % ($P < 0.001$). Using gray matter, patients with PSP were detected with a total accuracy of 86 % as well, however, with a sensitivity of 82 % and a specificity of 91 % ($P < 0.005$). Interestingly, the highest accuracies were obtained when using a restricted feature selection taking white matter in the midbrain into account (Fig. 5C). Here, we obtained a total accuracy of 98 % ($P = 0.0001$) showing only a single misclassified patient and no misclassified control. Note, in a comparison of the two groups, the chance level is 50 %. Regions contributing to correct classification mirrored areas identified in the structural group comparison of the entire PSP group versus controls. Fig. 5 shows the weight of voxels with no applicable units, meaning that it refers to the distance of the features to the hyperplane. Additionally, we ran analyses on the ECM maps, however, showing no significant results ($P > 0.01$) (data shown in our repository, see PRoNTo.zip in osf.io/yan47/). Thus, in our cohort, ECM may not be a suitable measure for predicting PSP, whereas structural MRI yielded a significant classification accuracy.

4. Discussion

We comprehensively describe brain alterations in patients with PSP underlining the involvement of both widespread structural and functional connectivity changes. Our study identified extensive gray/white matter volume differences (lower) in regions also known as pathognomonic markers such as the midbrain and cerebellar penduculi. Beyond that, thinner gray matter in the cingulate cortex, medial/temporal gyrus, and insula were found. Patients with PSP were characterized by less interconnectedness in the left frontal and supramarginal areas as well as in the right cingulate and frontal cortices. Stronger functional connectivity was found bilaterally in the cingulate, frontal, and temporal gyri. Seed-based functional connectivity of disease-specific hubs, obtained by systematic meta-analyses [2], were stronger in the midbrain and weaker in insulae and right thalamus. Using machine learning, we correctly predicted patients with PSP based on gray and white matter alterations with up to 86 % accuracy. Restricting feature selection including the midbrain only, accuracy was increased to 98 % showing only a single misclassified patient in our analysis. Contrarily, functional

Seed-based connectivity

$P < 0.05$ FWE

PSP< HC ⬤ PSP> HC ⬤
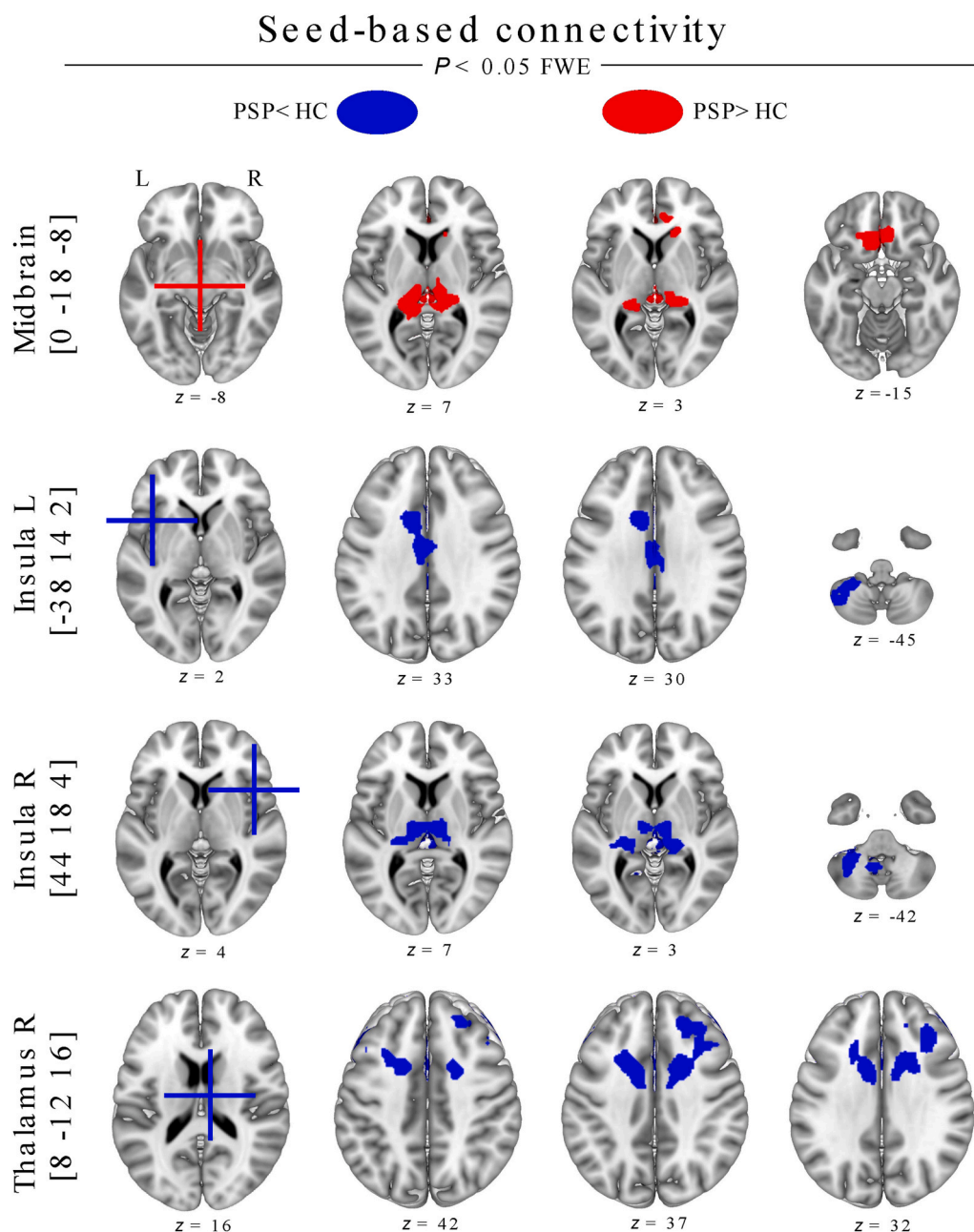
Fig. 4. Seed-based connectivity analysis in patients with progressive supranuclear palsy (PSP) compared with healthy controls (HC). Weaker and stronger functional connectivity are shown for each seed. Seeds were chosen according to disease-prototypical atrophy identified by our comprehensive meta-analysis in a large independent cohort [2]. Slice coordinates (z) in mm. Abbreviations: FWE family-wise error correction, L left, R right.

connectivity data did not lead to satisfactory classification accuracies showing no significant result. The observed changes matched the expectations derived from the existing body of the literature. The present study adds to the literature by providing a comprehensive, multimodal description of the orphan disease PSP, investigated in a reasonably sample-sized cohort of patients with PSP.

4.1. Structural brain alterations in PSP underline the importance of the midbrain beyond additional brain regions

Our study identified widespread gray and white matter alterations in PSP, including areas we recently identified as disease-related in a meta-analysis [2]. In the present study, gray matter atrophy was evident in the following regions: bilateral thalami, bilateral anterior insulae, midbrain, and left caudate nucleus. Regarding the white matter, atrophy was observed in the bilateral cerebral and
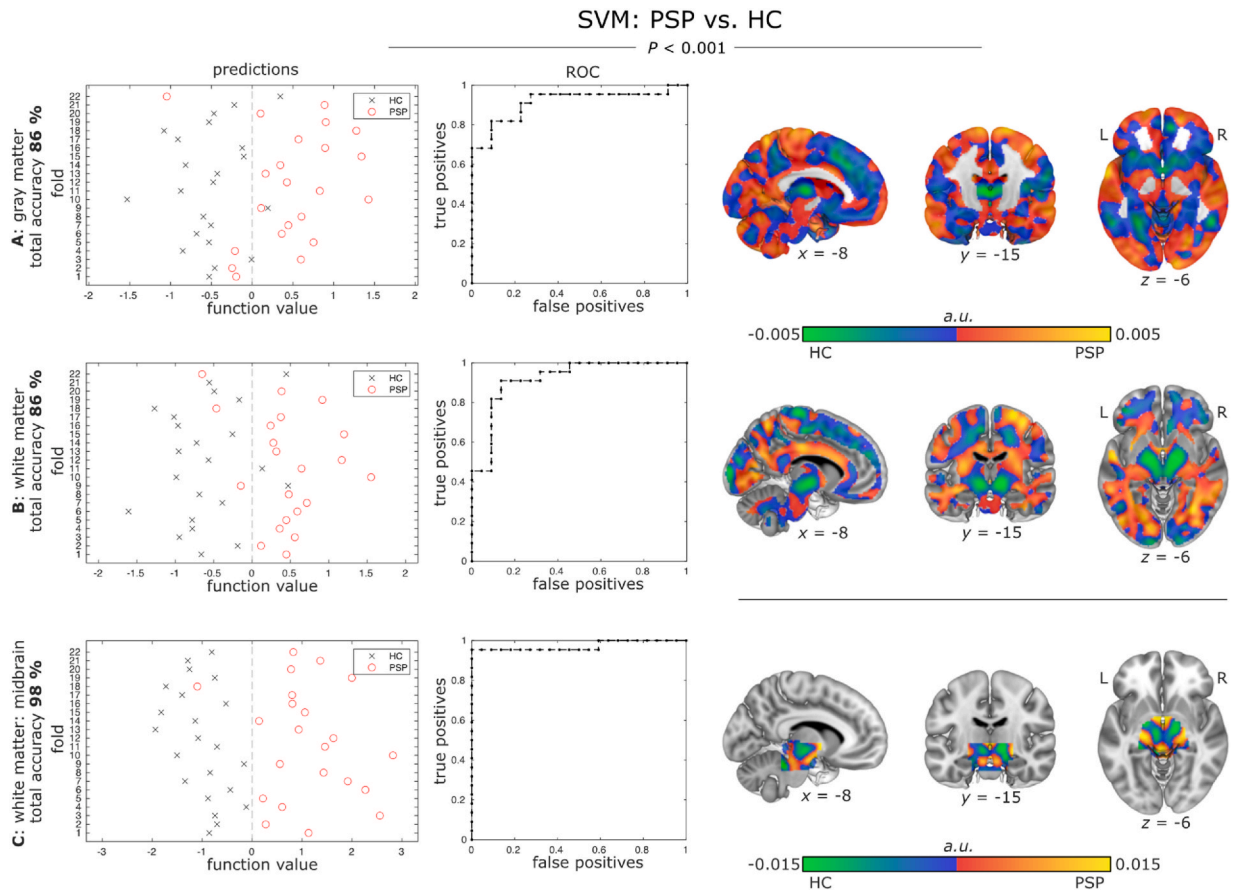
Fig. 5. Multivariate pattern analyses of structural gray and white matter using support vector machine classification (SVM). **A**: gray matter classification, **B**: white matter classification, and **C**: midbrain classification. Left panel: individual prediction of patients with progressive supranuclear palsy (PSP) and healthy controls (HC). Middle panel: receiver operating characteristic (ROC) curves for PSP diagnosis based on structural imaging data. Right panel: Weights of voxels most relevant for individual classification. Note that these weights are relative and have no applicable units (a. u.). Slice coordinates (x,y,z) in mm. Abbreviations: L left, R right.

cerebellar peduncles, midbrain, and right thalamus. It is not a contradiction that the present study found more extensive alterations than our recent meta-analysis. Due to differences between these two statistical approaches, results differ in the sense that the meta-analyses are more focal than VBM results since they only consider local maxima from respective studies and not whole clusters.

Nevertheless, it is important that we could replicate the findings of the meta-analysis in the present cohort. The diagnostic criteria for PSP [1] mention midbrain atrophy only as a supportive criterion. Our study suggests once again the potential importance of the midbrain, which has been shown to even differentiate PSP from other Parkinsonian syndromes [2,17]. White matter volume has not yet been intensively studied in PSP. Even though Rosskopf et al. [6] investigated white matter volume, they only found total gray matter volume to be lower in patients with PSP.

Concerning cortical thickness, Worker et al. [18] observed thinner cortex in the precentral, superior frontal, and lateral orbitofrontal gyri in patients with PSP. However, Agosta et al. [19] identified thinner cortex in medial/dorsolateral frontal, temporoparietal, and occipital areas, which is partially in line with our results in medial and temporal regions. Note that the aforementioned studies were based on 1.5T MRI and smaller cohorts, which might be a reason for deviating results.

4.2. Hypoconnectivity in PSP is accompanied by presumed compensatory hyperconnectivity

The goal of functional connectivity analyses is to identify how signals from spatially distinct brain regions co-vary. To date, the majority of studies have investigated local and hypothesis-driven changes in interconnectedness in patients with PSP. Our application of data-driven, whole-brain ECM analysis identified weaker connectivity in the left frontal and supramarginal areas as well as in the right cingulate and frontal cortices. Stronger functional connectivity was observed bilaterally in the cingulate, frontal, and temporal cortices. Notably, we identified both, weaker and stronger functional connectivity in patients with PSP.

Our results are in line with a selective functional connectivity study in PSP, which found weaker prefrontal cortex connectivity and stronger midbrain to thalamus connectivity [6]. In a review, Hillary et al. [20] demonstrated that increased local and whole-brain

functional connectivity is essential for compensation and thus, a frequent response to neurological diseases. They further highlight that hypo- and hyper-connectivity are not contradictory and common to find both together. This is further seen in an ECM study in corticobasal syndrome, another atypical Parkinsonian syndrome and tauopathy, where weaker and stronger functional connectivity were found simultaneously [21]. Weaker functional connectivity was detected in the right temporoparietal/insular regions and stronger in the frontal cortex and bilateral caudate nuclei. Regions with strong functional connectivity were similar to our obtained hyper-connected areas but weak connectivity differed between the diseases. This may suggest that stronger functional connectivity is due to compensatory efforts, which might be similar in both tauopathies, i.e., corticobasal syndrome and PSP, even though the diseases affect different regions in the brain.

In our meta-analytically informed functional connectivity analyses, patients with PSP were characterized by stronger functional connectivity of the midbrain and weaker functional connectivity of the insulae and right thalamus, which is in agreement with other studies on seed-based functional connectivity. Gardner et al. [3] reported intrinsic network disruption in patients with PSP in the dorsal midbrain network when placing seeds in the brainstem, basal ganglia, diencephalic, and cerebellar regions. Interestingly, these nodes are also known to exhibit atrophy and tau aggregation in PSP. Additionally, thalamocortical connectivity differences were identified in patients with PSP in a seed-based study by Whitwell et al. [4]. Bharti et al. [5] showed in an independent component analysis that within-network functional connectivity was stronger in the default mode network and cerebellum in patients with PSP. Further, between-network functional connectivity was weaker between the visual and auditory network and between the cerebellum and insula.

4.3. Structural imaging is superior to eigenvector centrality mapping in predicting PSP individually by machine learning

We have demonstrated that whole-brain changes can differentiate patients with PSP from healthy controls at a single-subject level by means of SVM. While the models for whole-brain structural alterations showed significant classification with accuracies around 86 %, models with restricted feature selection using the midbrain (white matter) yielded an accuracy up to 98 %. In contrast to these structural analyses, SVM classification with eigenvector centrality mapping did not show any significant result. This suggests that for our cohort structural alterations were more specific in describing the disease than ECM measures. Interestingly, after building another classifier based on atlas-based weights, the midbrain was excellent in predicting PSP. One may have expected the midbrain as the most important brain region, since it is known as a pathognomonic marker.

Our classification results did not improve when including more information about the disease using rs-fMRI in addition to structural MRI. This is noteworthy given that in a recent study we showed that in patients with corticobasal syndrome, classification results slightly, but not significantly, improved by adding rs-fMRI information when building the classifier [21]. Even though more information helps to understand and describe the disease, it might be that in the case of machine learning, it is not beneficial and adds the risk of overfitting. Interestingly, a recent study showed a significant classification between PSP and healthy controls based on pure gray matter alterations [22], however, as PSP is dominantly located in the white matter, we included gray and white matter volumes into classification and obtained much higher accuracies.

4.4. Study limitations

Our study identified consistent structural and functional connectivity changes enabling individual classification in PSP, but we acknowledge several limitations. Although our sample of patients with PSP might be regarded as small at first glance, PSP is regarded as a rare or orphan disease. Our multicentric design actually allowed a reasonable number of patients to be included. We recognize that the robustness of research findings is often correlated with sample size. However, given the rare nature of PSP, recruiting a large sample presents significant challenges. Our study aimed to provide preliminary insights into the brain imaging characteristics of patients with PSP. Still, especially the machine learning analysis need to be interpreted with caution and should be ideally replicated in bigger samples. Due to the different sites, different scanners have been used, which may influence the results. Possible biases due to the multicentric approach were reduced by using only 3T MRI and homogenously applied Siemens MAGNETOM scanners. We compared our patients with PSP only to healthy controls. Adding further disease groups might be useful to test the specificity of our results since differentiating PSP from other Parkinsonian syndromes remains challenging. Further, there is evidence that PSP and Parkinson's disease actually do differ with respect to structural indices of the midbrain [2,17]. We applied hypothesis-free ECM to obtain whole-brain functional network organization, whereas previous connectivity studies applied ROI approaches, making the comparability of findings difficult. However, the potential benefits gained by identifying regions of difference outside previous used ROIs would seem to outweigh the limitation. We would like to highlight that our conclusions were made for ECM, other functional connectivity or graph theory measures might perform differently in the SVM analysis. Thus, further research should evaluate this. Furthermore, different functional connectivity analysis methods might provide subtlety different insights into network alterations in PSP. Nonetheless, our results need to be replicated with similar methods. We acknowledge further that the unavailability of diffusion tensor imaging and FLAIR images to incorporate structural connectivity and vascular pathology is a limitation. Finally, histopathological validation of PSP was not available in our cohort as well as a deeper description of the disease than disease duration and global cognition. Hence, even though experienced neurologists examined the patients, we cannot be sure if a misclassification is a lack of the machine learning algorithm or a lack of classification of the neurologist.

4.5. Conclusion

To conclude, patients with PSP exhibited alterations in both, brain structure and functional connectivity derived from multimodal MRI using data-driven and whole-brain approaches. We consistently identified the midbrain as affected, highlighting the relevance of this brain region as a pathognomonic marker. Beyond that, we found other brain regions seem to be altered by the disease such as the cerebellum needing further investigation and replication. Most remarkably, alterations in brain structure were found to be superior to functional connectivity imaging parameters, in particular for prediction with machine learning.

Study funding

CRediT authorship contribution statement

Franziska Albrecht: Writing – review & editing, Writing – original draft, Visualization, Validation, Software, Project administration, Methodology, Investigation, Formal analysis, Data curation, Conceptualization. **Karsten Mueller:** Writing – review & editing, Supervision, Resources, Methodology, Conceptualization. **Tommaso Ballarini:** Writing – review & editing, Methodology, Data curation. **Klaus Fassbender:** Resources, Data curation. **Jens Wiltfang:** Resources, Data curation, German FTLD-Consortium, Resources, Funding acquisition, Data curation. **Adrian Danek:** Writing – review & editing, Supervision, Resources, Project administration, Funding acquisition, Data curation, Conceptualization. **Robert Jech:** Resources, Project administration, Funding acquisition, Data curation. **Mattias L. Schroeter:** Resources, Project administration, Funding acquisition, Data curation.

Declaration of competing interest

The authors declare that they have no known competing financial interests or personal relationships that could have appeared to influence the work reported in this paper.

Acknowledgments

Appendix A. Supplementary data

Supplementary data to this article can be found online in the OSF repository osf.io/yan47/.

References

[1] G.U. Höglinger, et al., Clinical diagnosis of progressive supranuclear palsy: the movement disorder society criteria, Movement Disorders 32 (2017) 853–864.
[2] F. Albrecht, S. Bisenius, J. Neumann, J. Whitwell, M.L. Schroeter, Atrophy in midbrain & cerebral/cerebellar pedunculi is characteristic for progressive supranuclear palsy - a double-validation whole-brain meta-analysis, Neuroimage Clin 22 (2019) 101722, https://doi.org/10.1016/j.nicl.2019.101722.
[3] R.C. Gardner, et al., Intrinsic connectivity network disruption in progressive supranuclear palsy, Ann. Neurol. 73 (2013) 603–616.
[4] J.L. Whitwell, et al., Disrupted thalamocortical connectivity in PSP: a resting-state fMRI, DTI, and VBM study, Parkinsonism & related disorders 17 (2011) 599–605.
[5] K. Bharti, et al., Abnormal resting-state functional connectivity in progressive supranuclear palsy and corticobasal syndrome, Front. Neurol. 8 (2017) 248.
[6] J. Rosskopf, et al., Intrinsic functional connectivity alterations in progressive supranuclear palsy: differential effects in frontal cortex, motor, and midbrain networks, Movement Disorders 32 (2017) 1006–1015, https://doi.org/10.1002/mds.27039.
[7] J. Bian, X. Wang, W. Hao, G. Zhang, Y. Wang, The differential diagnosis value of radiomics-based machine learning in Parkinson's disease: a systematic review and meta-analysis, Front. Aging Neurosci. 15 (2023), https://doi.org/10.3389/fnagi.2023.1199826.
[8] K. Mueller, J. Lepsien, H.E. Möller, G. Lohmann, Commentary: cluster failure: why fMRI inferences for spatial extent have inflated false-positive rates, Front. Hum. Neurosci. 11 (2017), https://doi.org/10.3389/fnhum.2017.00345.
[9] G. Flandin, K.J. Friston, Analysis of family-wise error rates in statistical parametric mapping using random field theory, Hum. Brain Mapp. 40 (2019) 2052–2054, https://doi.org/10.1002/hbm.23839.
[10] C. Gaser, R. Dahnke, CAT-a computational anatomy toolbox for the analysis of structural MRI data, HBM 2016 (2016) 336–348.
[11] J.D. Power, et al., Methods to detect, characterize, and remove motion artifact in resting state fMRI, Neuroimage 84 (2014) 320–341, https://doi.org/10.1016/j.neuroimage.2013.08.048.

[12] G. Lohmann, et al., LIPSIA—a new software system for the evaluation of functional magnetic resonance images of the human brain, Computerized medical imaging and graphics 25 (2001) 449–457.

[13] O. Perron, Zur Theorie der Matrices, Math. Ann. 64 (1907) 248–263, https://doi.org/10.1007/BF01449896.

[14] G. Goelman, N. Gordon, O. Bonne, Maximizing negative correlations in resting-state functional connectivity MRI by time-lag, PLoS One 9 (2014) e111554.

[15] K. Murphy, R.M. Birn, D.A. Handwerker, T.B. Jones, P.A. Bandettini, The impact of global signal regression on resting state correlations: are anti-correlated networks introduced? Neuroimage 44 (2009) 893–905.

[16] J. Schrouff, et al., PRoNTo: pattern recognition for neuroimaging toolbox, Neuroinformatics 11 (2013) 319–337.

[17] J.L. Whitwell, et al., Radiological biomarkers for diagnosis in PSP: where are we and where do we need to be? Movement Disorders 32 (2017) 955–971.

[18] A. Worker, et al., Cortical thickness, surface area and volume measures in Parkinson's disease, multiple system atrophy and progressive supranuclear palsy, PLoS One 9 (2014) e114167.

[19] F. Agosta, et al., Tracking brain damage in progressive supranuclear palsy: a longitudinal MRI study, J. Neurol. Neurosurg. Psychiatr. 89 (2018) 696–701.

[20] F.G. Hillary, et al., Hyperconnectivity is a fundamental response to neurological disruption, Neuropsychology 29 (2015) 59.

[21] T. Ballarini, et al., Disentangling brain functional network remodeling in corticobasal syndrome - a multimodal MRI study, Neuroimage Clin 25 (2020) 102112, https://doi.org/10.1016/j.nicl.2019.102112.

[22] K. Mueller, et al., Disease-specific regions outperform whole-brain approaches in identifying progressive supranuclear palsy: a multicentric MRI study, Front. Neurosci. 11 (2017), https://doi.org/10.3389/fnins.2017.00100.